

# Supporting Information

## Electronic transport descriptors for the rapid screening of thermoelectric materials

Tianqi Deng<sup>1\*</sup>, Jose Recatala-Gomez<sup>2,3\*</sup>, Masato Ohnishi<sup>4\*</sup>, D. V. Maheswar Repaka<sup>3\*</sup>, Pawan Kumar<sup>3</sup>, Ady Suwardi<sup>3</sup>, Anas Abutaha<sup>3,5</sup>, Iris Nandhakumar<sup>2</sup>, Kanishka Biswas<sup>6</sup>, Michael B. Sullivan<sup>1</sup>, Gang Wu<sup>1</sup>, Junichiro Shiomi<sup>4#</sup>, Shuo-Wang Yang<sup>1#</sup>, Kedar Hippalgaonkar<sup>3,7#</sup>

\* Denotes equal contribution, # Corresponding author

<sup>1</sup> Institute of High Performance Computing, Agency for Science, Technology and Research (A\*STAR), 1 Fusionopolis Way, Singapore 138632, Republic of Singapore

<sup>2</sup> Department of Chemistry, University of Southampton, University Road, Highfield, Southampton SO17 1BJ, United Kingdom

<sup>3</sup>Institute of Materials Research and Engineering, Agency for Science, Technology and Research (A\*STAR), 2 Fusionopolis Way, Singapore 138634, Republic of Singapore

<sup>4</sup>Department of Mechanical Engineering, The University of Tokyo, Hongo 7-3-1, Bunkyo-ku, Tokyo 113-8656, Japan

<sup>5</sup>Qatar Environment and Energy Research Institute, Hamad Bin Khalifa University, Qatar Foundation, Doha, 34110, Qatar

<sup>6</sup>New Chemistry Unit and School of Advanced Materials and International Centre for Materials Science, Jawaharlal Nehru Centre for Advanced Scientific Research (JNCASR), Bangalore 560064, India

<sup>7</sup>School of Material Science and Engineering, Block N4.1, 50 Nanyang Avenue, Nanyang Technological University, Singapore 639798, Republic of Singapore

### Corresponding Authors

#E-mail: [kedar@ntu.edu.sg](mailto:kedar@ntu.edu.sg), [yangsw@ihpc.a-star.edu.sg](mailto:yangsw@ihpc.a-star.edu.sg), [shiomi@photon.t.u-tokyo.ac.jp](mailto:shiomi@photon.t.u-tokyo.ac.jp)

## Supplementary Section 1: Detailed derivation of the mobility descriptor

The scattering rate (Figure 3) is dominated by ionised impurities (IIS) with a non-negligible contribution from polar optical phonons (POP). We start by considering the charge carrier scattering rate due to polar optical phonons ( $\tau_{POP}$ )<sup>1,2</sup>:

$$\frac{1}{\tau_{POP}} = C_{POP}^2 \frac{\Omega}{\pi \hbar} \sqrt{\frac{m_s(E)}{2E}} \left\{ \sinh^{-1} \sqrt{\frac{E}{\hbar \omega}} [\beta(\hbar \omega, T) + f(E + \hbar \omega - \zeta, T)] + \sinh^{-1} \sqrt{\frac{E}{\hbar \omega}} [\beta(\hbar \omega, T) + f(E - \hbar \omega - \zeta, T)] \right\} \quad (S1)$$

where  $C_{POP}^2$  is the angular averaged Fröhlich coupling strength,  $\Omega$  is the unit cell volume,  $\hbar$  is the reduced Planck constant,  $m_s(E)$  is the average energy-dependent effective mass from band curvature calculation,  $E$  is the energy relative to the band edge,  $\omega$  is the phonon frequency,  $T$  is the absolute temperature,  $\beta$  is the Bose-Einstein distribution function for phonons,  $f$  is the Fermi-Dirac distribution of electrons and  $\zeta$  is the chemical potential.<sup>2</sup> Since the angular averaged Fröhlich coupling strength is inversely proportional to the dielectric constant ( $\epsilon$ ), we conclude that the scattering rate due to POP will be directly proportional to the square of the dielectric constant:  $C_{POP} \propto \epsilon^{-1}$ ,  $\tau_{POP}(E) \propto \epsilon^2$ .

On the other hand, the charge carrier scattering rate due to ionised impurities ( $\tau_{IIS}$ ) is given by:

$$\tau_{IIS}(E) = \frac{16 \sqrt{2m^*} \pi \epsilon^2 \epsilon_0^2}{N_I q^4} \left[ \ln(1 + \gamma^2) - \frac{\gamma^2}{1 + \gamma^2} \right]^{-1} E^{\frac{3}{2}} \quad (S2)$$

where  $1/\tau_{IIS}$  is the scattering rates dominated by ionised impurities<sup>3</sup>,  $N_I$  is the number of impurities,  $q$  is the elemental charge,  $m^*$  is the DOS effective mass (or Seebeck mass,  $m_s$ ),  $\epsilon$  is the dielectric constant,  $\epsilon_0$  is the vacuum permittivity and  $\gamma$  is described in Equation S3:

$$\gamma = \frac{8m^* E(p) L_D^2}{\hbar} \quad (S3)$$

where  $L_D$  is the Debye length,  $\hbar$  is the reduced Planck constant and  $E(p)$  is a momentum dependent energy function.<sup>3</sup> Directly from Equation S2, we observe that the scattering due to ionised impurities is directly proportional to the square of the dielectric constant:  $\tau_{IIS}(E) \propto \epsilon^2$ . Hence, we conclude that the scattering rates due to IIS and POP are proportional to the square of the dielectric constant.

Regarding the density-of-states effective mass, the correlation is not as straightforward. The POP scattering rate time is inversely proportional to the square root of effective mass  $\tau_{POP}(E) \propto m^{-1/2}$  (Equation S1) while the weakly screened impurity scattering time is directly proportional to  $m^{1/2} N_I^{-1}$  (Equation S2). However, as the impurity and carrier densities increase, the additional dependence on

effective mass is introduced through the Debye screening length,  $L_D \approx \sqrt{\frac{\epsilon\epsilon_0 k_B T}{e^2 n}}$ . In the high-density limit, impurity scattering time becomes proportional to  $\tau_{IIS}(E) \propto N_I^{-1} L_D^{-4} D^{-1}(E) \propto N_I^{-1} n^2 m^{-3/2}$  instead<sup>3</sup>, where  $D(E)$  is the density of states and  $n$  is the carrier density. Since the optimal doping level, as discussed in the main text, is proportional to  $m_s^{3/2}$ , the impurity scattering rate no longer depends on effective mass. Since both POP scattering and impurity scattering are important in this case, the scattering time should have an effective mass dependence that is weaker than  $m_s^{-1/2}$ . Therefore, we choose to drop this weak but complex dependency and focus on the more significant factor, *i.e.* the dielectric constant.

**Table S1:** Summary of low optical phonon frequencies for the 12 ABX<sub>2</sub> materials resulting of the data mining and subsequent filtering.

Chemical formula	Low optical phonon frequency
AgBiS <sub>2</sub>	Yes, Ag and Bi (ca. 50 cm <sup>-1</sup> ).
CrAuS <sub>2</sub>	Yes, Au (ca. 50 and 100 cm <sup>-1</sup> ).
KCrS <sub>2</sub>	Yes, K around 110 cm <sup>-1</sup>
TlBiS <sub>2</sub>	Yes, Bi and Tl around 50 cm <sup>-1</sup>
NaCrSe <sub>2</sub>	No (Na around 125 cm <sup>-1</sup> )
NaInSe <sub>2</sub>	Yes, Na around 79 cm <sup>-1</sup>
ScTlSe <sub>2</sub>	Yes, Tl below 50 cm <sup>-1</sup>
TlBiSe <sub>2</sub>	Yes, Bi and Tl below 50 cm <sup>-1</sup>
GdTlTe <sub>2</sub>	Yes. Tl around 30 cm <sup>-1</sup> . Ga and Te have similar PhDOS around 50 cm <sup>-1</sup>
KGdTe <sub>2</sub>	Yes, Ga around 50 cm <sup>-1</sup> but is not as prominent
TlBiTe <sub>2</sub>	Yes, Bi and Tl below 50 cm <sup>-1</sup>
TlSbTe <sub>2</sub>	Yes, Tl around 30 cm <sup>-1</sup> , Sb and Te around 50 cm <sup>-1</sup>

**Table S1.** Survey of low frequency phonon states in the data.

**Figure S1:** Extended data on the thermal conductivities of ABX<sub>2</sub> compounds.

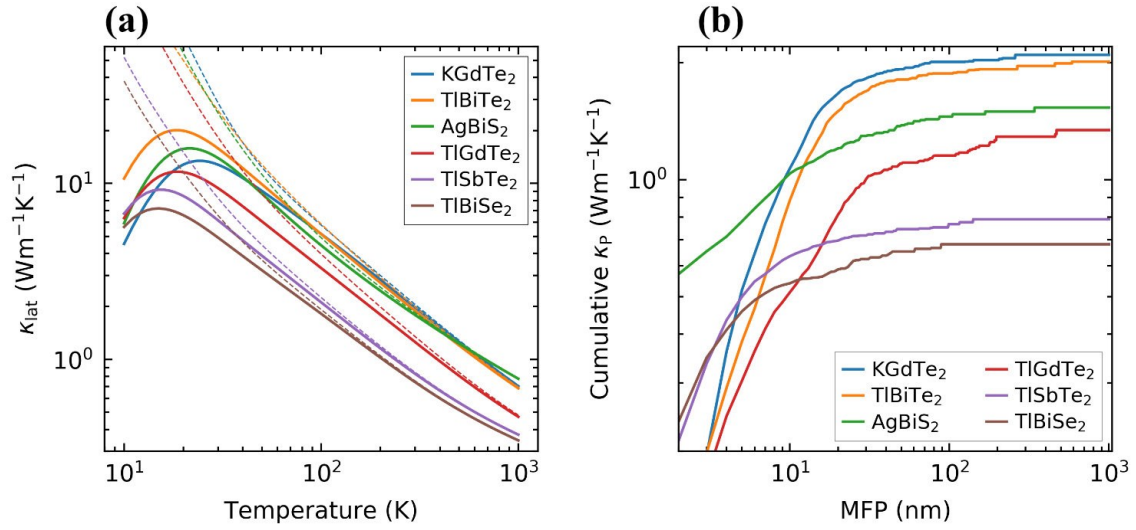


**Figure S1.** Thermal conductivities of ABX<sub>2</sub> compounds. (a) Temperature-dependent thermal conductivities for all the analysed materials. Both of the population (Peierls) and coherence contributions are considered. Dotted and solid lines show data for single crystals and polycrystals with 1 μm grain size, respectively. (b) Cumulative thermal conductivities for population contribution with respect to phonon mean-free-path (MFP) at 300 K.

**Figure S2:** Relationship between the direction averaged powerfactor and the Fermi surface complexity factor ( $N_V^*K^*$ ).<sup>4</sup>

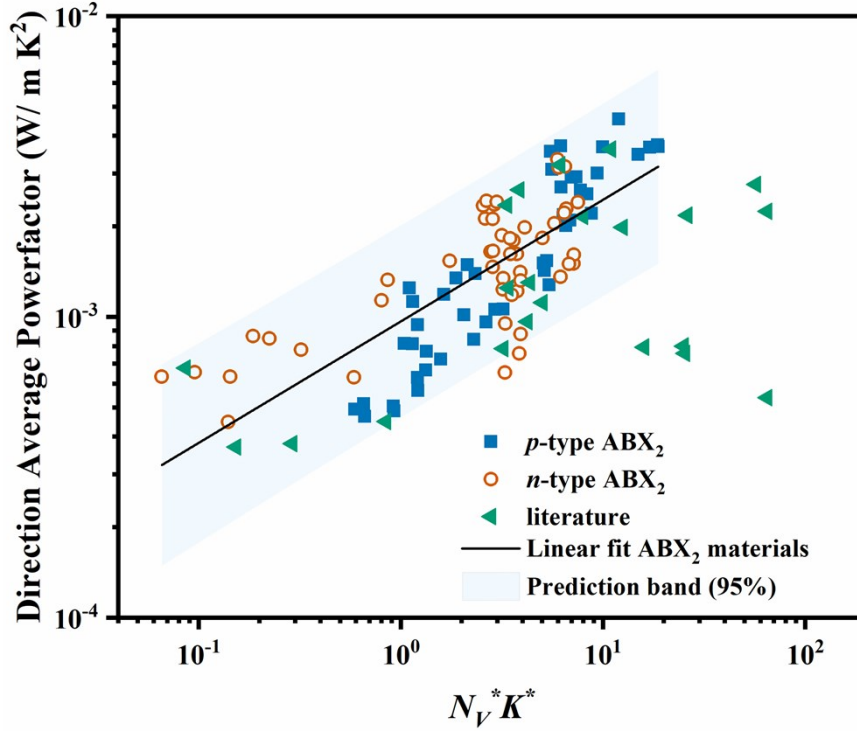


**Figure S2.** Direction average powerfactor for  $ABX_2$  compounds and literature values as a function of the Fermi surface complexity factor ( $N_V^*K^*$ ).<sup>4</sup> The blue area corresponds to the prediction band calculated for  $ABX_2$  compounds. It corresponds to the range of values that are likely to contain the value of a new observation, with a 95% confidence.

The transport descriptor for the powerfactor (Equation 3 in the main text) can be expressed in terms of

the Fermi surface complexity factor by equating  $N_V^*K^*$  to  $\left(\frac{m_S}{m_C}\right)^{1.5}$ . This is given by Equation S4:

$$PF \propto \varepsilon^2 (N_V^*K^*)^{2/3} m_S^{0.5} T^{1.5} \quad (S4)$$

In Equation S4, the dielectric constant ( $\varepsilon$ ) relates to the interaction strength,  $N_V^*K^*$  comes from the complexity of the bandstructure and the Seebeck mass ( $m_S^{0.5}$ ) and temperature dependence ( $T^{1.5}$ ) arise from the optimal carrier concentration assumption.



**Figure S3:** Further information on phonon relaxation time of TA mode at T point of both pristine AgBiS<sub>2</sub> and AgBiS<sub>2</sub> under 0.5% hydrostatic strain.

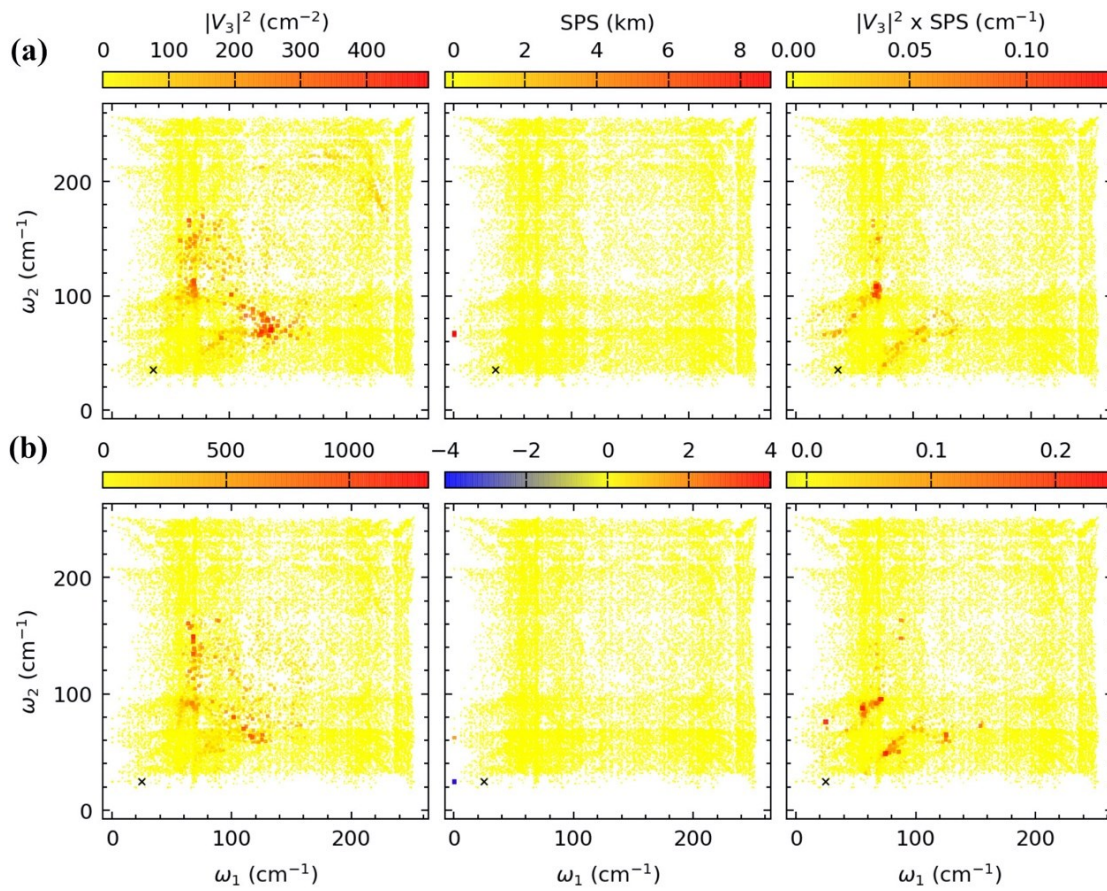


**Figure S3.** Detailed information on phonon relaxation time ( $|V_3|^2$ , SPS, and  $|V_3|^2 \times SPS$ ) of TA mode at T point of AgBiS<sub>2</sub> for (a) the pristine structure and (b) the structure under 0.5% hydrostatic strain. The frequency of the TA mode is shown by the cross (x).

**Figure S4:** Temperature and carrier nature dependence of the direction averaged powerfactor for ABX<sub>2</sub> materials. Note that the powerfactor is at optimal carrier concentration.

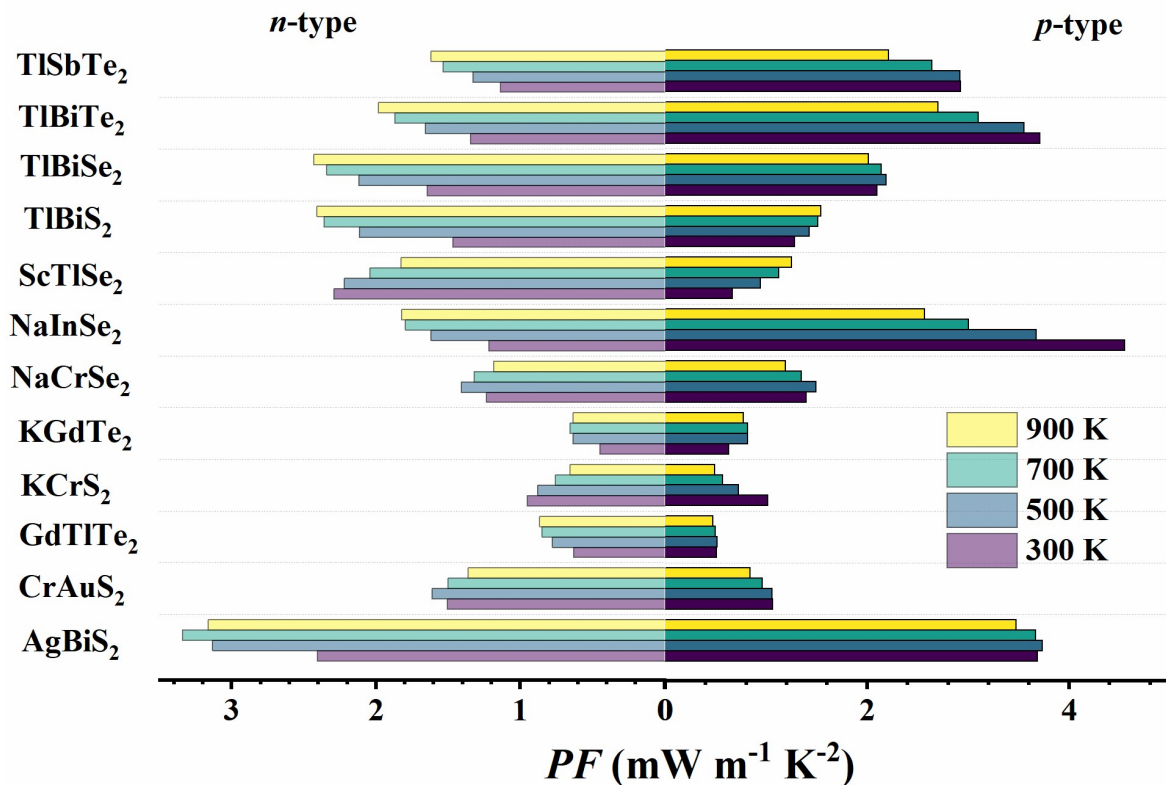


**Figure S4.** Direction-average powerfactor, at optimal carrier concentration, as a function of temperature for both *n*- and *p*-type ABX<sub>2</sub> chalcogenides.

## References

- 1 C. Verdi and F. Giustino, *Phys. Rev. Lett.*, 2015, **115**, 176401.
- 2 T. Deng, G. Wu, M. B. Sullivan, Z. M. Wong, K. Hippalgaonkar, J.-S. Wang and S.-W. Yang, *npj Comput. Mater.*, 2020, **6**, 46.
- 3 M. Lundstrom, *Fundamentals of Carrier Transport*, Cambridge University Press, Cambridge, 2000.
- 4 Z. M. Gibbs, F. Ricci, G. Li, H. Zhu, K. Persson, G. Ceder, G. Hautier, A. Jain and G. J. Snyder, *npj Comput. Mater.*, 2017, **3**, 1–6.